



FULL PAPER

Platinum-Imidazolyl Schiff Base Complexes Immobilized in Periodic Mesoporous Organosilica Frameworks as Catalysts for Hydrosilylation

Yingpeng Huo^{1,2,3,4,5} | Jiwen Hu^{1,2,3,4,5} | Yuanyuan Tu^{1,2,5} |
Zhenzhu Huang^{1,2,5} | Shudong Lin^{1,2,5} | Yangfei Hu^{1,2,5} | Chao Feng^{1,2,5}

¹Guangzhou Institute of Chemistry, Chinese Academy of Sciences, Guangzhou, 510650, P.R. China

²The University of Chinese Academy of Sciences, Beijing, 100039, P.R. China

³Guangdong Provincial Key Laboratory of Organic Polymer Materials for Electronics, 510650, P.R. China

⁴CAS Engineering Laboratory for Special Fine Chemicals, 510650, P.R. China

⁵CASH GCC (Nanxiong) Research Institute of New Materials Co., Ltd, 512400, P.R. China

Correspondence

Prof. Dr. Jiwen Hu, Guangzhou Institute of Chemistry, Chinese Academy of Sciences, Guangzhou, P. R. China, 510650. Email: hjw@gic.ac.cn

Funding information

National Natural Science Foundation of China, Grant/Award Numbers: 21404121, 21404122, 51173204, 51503124; Natural Science Foundation of Guangdong Province, Grant/Award Number: 2018A030313946; the Guangzhou Industrial Technology Major Project, Grant/Award Number: 201802010018; the Innovative Talents Youth Program (Natural Science) in Universities of Guangdong, Grant/Award Number: 2017-GKQNCS113; the Production Education Research Project in Guangdong Province, Grant/Award Number: 2015B090915004; the Science and Technology Program of Guangzhou City, Grant/Award Numbers: 201802010018, 201904020019; the Sichuan Science and Technology Project, Grant/Award Number: 2019YFSY0011

Abstract

An imidazolyl Schiff base-containing periodic mesoporous organosilica (PMO) was synthesized via co-condensation reactions between a newly prepared bis(imidazolyl)imine-bridged bis silane and tetraethyl orthosilicate in the presence of cetyltrimethyl ammonium bromide as a soft template. The resultant as-synthesized PMO was then employed as a solid support for platinum catalysts. This complex was fully characterized via various techniques including FTIR, solid-state ¹³C NMR, and ²⁹Si-NMR spectroscopy, as well as N₂ adsorption/desorption analysis, X-ray diffraction (XRD), X-ray photoelectron spectroscopy (XPS), scanning electron microscopy (SEM), and transmission electron microscopy (TEM) methods. In addition, the catalyst was proven to efficiently mediate hydrosilylation reactions between olefins and hydrosilanes, and it can be reused for at least five cycles without significant loss of activity.

KEYWORDS

hydrosilylation reactions, imidazolyl Schiff base, periodic mesoporous organosilica, platinum catalysts

1 | INTRODUCTION

Hydrosilylation reactions between carbon-carbon double bonds and hydrosilanes are one of the most important reactions in silicon chemistry and in industry,^[1] particularly with the frequent use of homogenous platinum

catalysts such as Speier's,^[2] Karstedt's,^[3] and later examples of Marko's catalysts.^[4] However, homogeneous platinum catalysts generally suffer from various drawbacks such as the formation of inactive aggregates, the need for tedious complex separation procedures,^[5] and discoloration of the final products,^[6] prompting the interest in

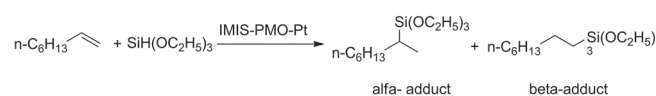
developing heterogeneous platinum catalysts that can be readily reused and recycled.^[7]

Periodic mesoporous organosilicas (PMOs) are one of the most widely investigated classes of inorganic–organic hybrid materials.^[8] PMOs can be prepared via the condensation of bis-silane compounds ((R₁O)₃Si-R-Si-(OR₁)₃, where R₁ = Me or Et), with or without tetraethyl orthosilicate (TEOS), and thus a vast variety of organic moieties can be uniformly incorporated into the frameworks of these materials.^[9] Since the first report of PMOs in 1999, numerous innovative examples of these materials have been synthesized, bearing various R groups ranging from simple ethylene, phenylene to hydrocarbons, hetero-aromatic and metal complexes. Meanwhile, research on the applications of such PMOs has been extended to many fields such as adsorption, chemical separations, thin films, the biomedical sector, and especially catalysis.^[10,11]

The application of PMOs in catalysis is an attractive theme, as functional PMOs with homogeneously distributed binding sites within the silica matrix can be obtained through simple templated sol–gel processes via the careful design of ligands containing organosilica precursors. These PMOs are ideal solid supports for various metal complexes and metal nanoparticles. Notably, they offer distinct characteristics such as relatively short reactant diffusion lengths and high accessibility to active sites, so that active nanoparticles can be stabilized and uniformly dispersed, thus enhancing their catalytic activities.^[12] Consequently, the preparation of PMOs with suitable bridging ligands in the pore walls to support metal complexes as heterogeneous catalysts has become a hot topic.^[13–17]

Nitrogen-containing heterocyclic Schiff bases represent a major class of polydentate ligands and fulfil important applications in metal coordination.^[18,19] Among them, flexible imidazolyl Schiff bases have been widely used in the synthesis of various metal (e.g., Cu, Fe, Zn, Ru, etc.) complexes, most of which have been proven to be efficient catalysts.^[20–26] In fact, the imidazolyl moiety itself is a fine chelating agent towards platinum due to the electron donating N atoms on its rigid ring, and several platinum-imidazolyl complexes have been reported in the literature.^[27–30] When it is further converted into a Schiff base, its chelating ability is further enhanced as the number of donating atoms increase, thus increasing its ability to form platinum complexes.

Inspired by these facts, we herein design for the first time a novel bis (imidazolyl) Schiff base bridged bis-silane compound (Scheme 1, compound 3), and use it as



SCHEME 1 Synthetic route towards **IMIS-PMO-Pt(0)**

a building block to construct a novel periodic mesoporous organosilica via co-condensation with TEOS. While we are not aware of any reports on platinum-imidazolyl Schiff base complexes immobilized in PMO frameworks, there have only been a few reports describing the immobilization of platinum onto PMOs containing bis (pyridine)^[31,32] or imidazolyl ionic liquids.^[33] The platinum-imidazolyl Schiff base-containing PMO could be then reduced by NaBH₄, thus endowing the resultant PMO with a uniform dispersion of ultrafine platinum nanoparticles (1–2 nm). Moreover, we also demonstrate that both platinum-imidazolyl Schiff base complex-containing and the platinum nanoparticle-containing PMOs can efficiently mediate the hydrosilylation reactions between olefins and hydrosilanes. In addition, the platinum nanoparticle-containing PMOs exhibit desirable recyclability, demonstrating the potential applicability of these PMO materials in catalysis.

2 | MATERIALS AND METHODS

2.1 | Reagents and chemicals

All of the reagents which were used in this research were of analytical grade or better, unless stated otherwise. Styrene, alpha-methylstyrene, triethoxy (vinyl)silane, 1-octadecene, 1-cyclooctene, allylbenzene, vinylpyridine, allyl phenyl ether, methyl dimethoxy vinyl silane, cinnamyl alcohol, norbornene, methallyl alcohol, oct-1-en-3-ol, allyl glycidyl ether, γ -aminopropyl triethoxysilane, 1H-imidazole-4-carbaldehyde, diiodomethane, triethoxysilane and cesium carbonate were purchased from Aladdin Industrial Corporation (Shanghai, China). Ethanol, toluene, and hydrochloric acid were purchased from Tianjin Fuyu Fine Chemical Co., Ltd. (Tianjin, China). Lastly, CD₃OD and chloroform-*d* (CDCl₃) with TMS as an internal standard were purchased from J & K Co., Ltd. (Beijing, China).

2.2 | Instruments

NMR spectra of the hydrosilylation adducts were recorded using a Bruker 400 MHz spectrometer. Solid-state ¹³C and ²⁹Si NMR spectra were recorded using a Bruker 600 MHz spectrometer. X-ray powder diffraction (XRD) data were collected using a RIGAKU SmartLab diffractometer with Cu K α radiation. Fourier-transform infrared spectra were recorded with a Nicolet 6700 spectrophotometer. DR-UV-Vis spectra were obtained with a Cary-300 Ultraviolet–visible spectrophotometer. A Thermo Scientific K-Alpha instrument was used to

record the X-ray photoelectron spectra (XPS) of the catalyst. Scanning electron microscopy (SEM) and energy dispersive spectroscopy (EDS) data were collected with a Hitachi SU8010 system that was equipped with a HORIBA EMAX ENERGY module. Meanwhile, N₂ adsorption/desorption experiments were conducted using a Micromeritics TriStar II 3flex Surface Area and Porosity Instrument. The exact platinum contents in the catalysts were analyzed with a HK-9600 inductively coupled plasma (ICP) spectrometer. TEM images were obtained with a JEM-2100F system.

2.3 | Preparation of 1,1'-methylenebis(1*H*-imidazole-4-carbaldehyde) (**2**)

H-Imidazole-4-carbaldehyde (3.18 g, 33.1 mmol) was placed in a 250 ml round-bottom flask and dissolved in 80.0 ml of anhydrous ethanol. Subsequently, diiodomethane (4.50 g, 16.8 mmol) and CsCO₃ (12.4 g, 35.0 mmol) were added to the solution under magnetic stirring. The reaction was conducted under reflux for 24 hr and monitored by thin-layer chromatography (TLC). The mixture was then allowed to cool to room temperature and the solvent was removed via rotary-evaporation under vacuum. The crude products were purified via silica gel chromatography (eluent: dichloromethane-methanol = 10:1, v/v) and 1.67 g of **2** (yield 48.7%) was thus obtained as light-yellow crystals. ¹H NMR and ¹³C NMR spectra of **2** are provided in Figures S1-S3 in the Supporting Information (SI).

2.4 | Preparation of (*N,N'E,N,N'E*)-*N,N'*-((1,1'-methylenebis(1*H*-imidazole-4,1-diyl)) bis (methanyl ylidene)) bis (3-(triethoxysilyl)propan-1-amine) (**3**)

Briefly, 0.102 g (0.500 mmol) of 1,1'-methylenebis(1*H*-imidazole-4-carbaldehyde) (**2**) was dissolved in 2 ml of methanol in a 10 ml round bottom flask. Under vigorous stirring, 0.221 g (1.00 mmol) of γ -amino propyl triethoxysilane was added dropwise into the flask. The solution was stirred for 15 hr at room temperature and the reaction was monitored by TLC. After the reaction was complete (~100% conversion), the solvent was removed from the reaction mixture via rotary-evaporation under vacuum to yield the crude product **3**. The ¹H and ¹³C NMR spectra of **3** were recorded without further purification with the use of MeOD as the solvent (Figures S4-S6 in the SI).

2.5 | Preparation of IMIS-PMO

The imidazolyl Schiff base-containing periodic mesoporous organosilica (**IMIS-PMO**) was synthesized via surfactant-directed co-condensation as illustrated in Scheme 1. In a typical trial, hexadecyltrimethylammonium bromide (CTAB, 0.431 g, 1.08 mmol) was dissolved in 50 ml of an aqueous solution containing 42.3 mg (1.06 mmol) of NaOH. The mixture was magnetically stirred at a speed of 200 rpm and heated to 50 °C until the solution was clear. Subsequently, 2.10 g (10.0 mmol) of tetraethyl orthosilicate (TEOS) was slowly added to this solution. After 5 min, a 1 ml ethanol solution of **3** (containing 0.204 g, 1.00 mmol of compound **3**) was added dropwise to the reaction mixture. After 4 hr of stirring at 50 °C, the gel solution was aged at 80 °C for 24 hr. The pale yellow precipitate was filtered, washed thoroughly with ethanol and deionized water, and then dried under vacuum at 50 °C for 10 hr. Subsequently, CTAB was removed by refluxing the solid product in 100 ml of ethanol at 80 °C for 24 hr and then the product was filtrated, washed with ethanol, and dried under vacuum at 50 °C overnight, thus producing **IMIS-PMO**.

2.6 | Preparation of IMIS-PMO-PtCl₂

IMIS-PMO (0.500 g) was dispersed in 50 ml of ethanol via ultra-sonication. Subsequently, sodium *tert*-butoxide (0.112 g, 1.16 mmol) and 5 ml of a H₂PtCl₆·H₂O/isopropanol solution (0.05 M) were added, and the reaction was allowed to proceed for 6 hr at room temperature. The resultant light yellow powder was filtered, washed thoroughly with ethanol, and then dried under vacuum at 50 °C for 10 hr, giving 0.485 g **IMI-PMO-PtCl₂**.

2.7 | Preparation of IMIS-PMO-Pt(0)

The synthetic route of IMIS-PMO-Pt(0) was illustrated by scheme 1. Typically, **IMIS-PMO-PtCl₂** (0.400 g) was dispersed in 50 mL of ethanol via ultra-sonication. This mixture was then cooled to -5 °C and 143 mg (3.78 mmol) of NaBH₄ was added while the solution was magnetically stirred. The reaction was carried out at -5 °C for 2 hr and then allowed to proceed further at room temperature for another 4 hr. The resultant pale black powder was filtered, washed thoroughly with ethanol, dried under vacuum at 50 °C for 10 hr, thus giving 0.387 g **IMI-PMO-Pt(0)**.

2.8 | Hydrosilylation reactions

The catalytic activity of **IMIS-PMO-PtCl₂** and **IMIS-PMO-Pt(0)** were evaluated based on their ability to catalyze a model hydrosilylation reaction between 1-octene and triethoxysilane. The reaction was performed in a 25 mL round-bottom flask with a magnetic stirrer. Most commonly, 780 μL (5.00 mmol) of 1-octene and **IMIS-PMO-PtCl₂/IMIS-PMO-Pt(0)** were added into the flask and stirred at 60 °C for 0.5 hr, and then 925 μL (5.00 mmol) of triethoxysilane was added and the mixture was subsequently stirred for 2–6 hr. The resulting mixture was analyzed via ¹H NMR spectroscopy without further purification.

The recyclability of **IMIS-PMO-Pt(0)** was evaluated in terms of the conversion performance obtained after repeated use for several cycles. Briefly, 10.5 mg of the catalyst that had been suspended in 2.34 ml (15.0 mmol) of 1-octene was first preheated at 60 °C for 30 min, and then 2.775 ml (15.0 mmol) of trimethoxysilane was added before the reaction was allowed to proceed for another 2 hr. The catalyst was then collected via centrifugation at 15000 rpm. The supernatant was poured out and then the remaining catalyst was mixed with fresh 1-octene before a second reaction cycle was conducted via the same procedure as mentioned above. The products obtained from each cycle were subsequently analyzed via ¹H NMR spectroscopy.

3 | RESULTS AND DISCUSSION

3.1 | Characterization of **IMIS-PMO**, **IMIS-PMO-PtCl₂**, and **IMIS-PMO-Pt(0)**

3.1.1 | The composition of **IMIS-PMO**, **IMIS-PMO-PtCl₂**, and **IMIS-PMO-Pt(0)**

The incorporation of the imidazole imine moiety within the pore walls of the resulting PMO was demonstrated by FTIR and solid-state NMR analysis. In the FTIR spectra of **IMIS-PMO**, **IMIS-PMO-PtCl₂**, and **IMIS-PMO-Pt(0)** (Figure S7 in the SI), the absorption bands at ~1062, 790, and 465 cm^{-1} corresponded to the Si-O-Si vibration.^[34] The bands at 2934 and 1467 cm^{-1} respectively corresponded to the stretching and bending vibrations of the $-(\text{CH}_2)_3-$ moieties.^[35] The small bands in the spectrum of **IMIS-PMO** at 1498 cm^{-1} represented the skeleton vibration of the imidazole ring, while those at 1336 and 1359 cm^{-1} showed the bending vibrations of C=N (Figure S8 in the SI),^[36] and these three peaks became weaker in the spectra of **IMIS-PMO-PtCl₂** and **IMIS-PMO-Pt(0)**, which might be due to

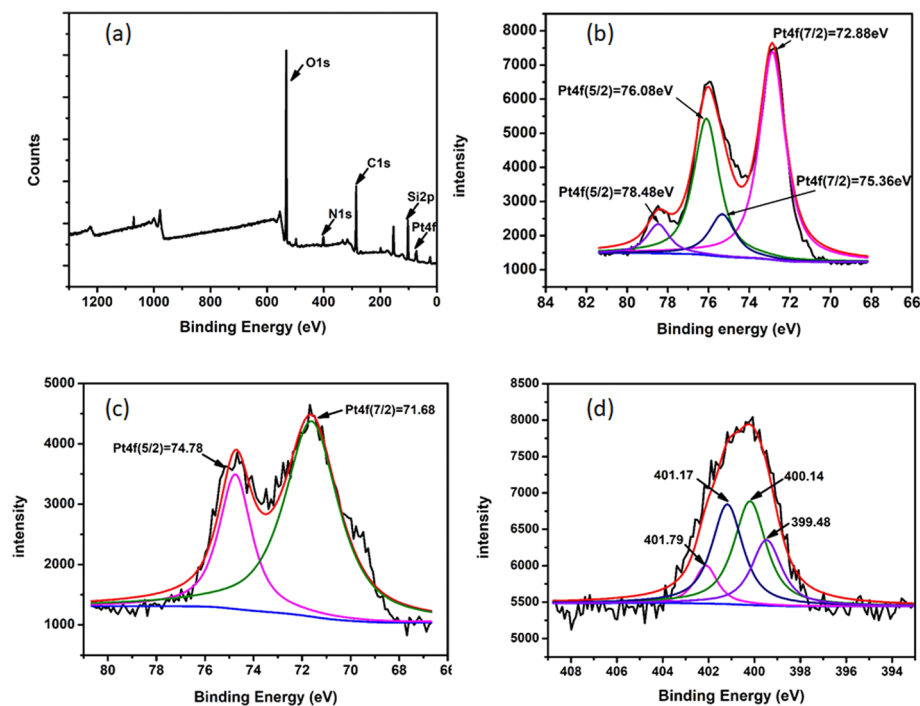
the binding effect between platinum and the N atom on the imidazole ring.

Further evidence could be found in the solid-state ¹³C and ²⁹Si NMR spectra of **IMIS-PMO**. As shown in Figure S9 (SI), the ¹³C NMR peaks at 164.9, 135.7, and 110.5 ppm corresponded to the imidazole imine moiety, while the peaks at 42.2, 20.8 and 9.7 ppm represented the carbons in the propyl chain.^[36,37] The peak at 61.4 ppm can be assigned to the $-\text{CH}_2-$ between the two imidazole ring and the peak at 191.5 ppm corresponded to the C=N.

The ²⁹Si NMR spectrum (Figure S10 in the SI) of **IMIS-PMO** displayed three resonance peaks corresponding to Q⁴ (Si (OSi)₄, $\delta = -89.3$ ppm), Q³ (Si (OSi)₃OH, $\delta = -80.5$ ppm), and Q² (Si (OSi)₂(OH)₂, $\delta = -71.5$ ppm), as well as T¹ signal ($-\text{CH}_2-\text{Si}(\text{OSi})(\text{OH})_2$) at $\delta = -44.9$ ppm, T² signal ($-\text{CH}_2-\text{Si}(\text{OSi})_2(\text{OH})$) at $\delta = -53.3$ ppm and T³ signal ($-\text{CH}_2-\text{Si}(\text{OSi})_3$) at $\delta = -61.3$ ppm.^[35] The presence of the Q^{*n*} (*n* = 2–4) peaks resulted from the self-condensation of TEOS. Meanwhile, the appearance of the T^{*n*} (*n* = 1–3) peaks can be attributed to the co-condensation between TEOS and compound **3**, which led to the covalent incorporation of imidazole imine moieties into the silica network. However, the T² or T³ signals were relatively weaker than the T¹ in the ²⁹Si Spectrum. This might be due to the comparatively slow stirring speed during the co-condensation reaction between TEOS and compound **3**, which may have resulted in insufficient condensation between the two hydrolyzed substrates.

The immobilization of platinum into the **IMIS-PMO** framework was then characterized by XPS. The XPS survey spectrum (Figure 1a) verified the presence of platinum within the resulting material. The Pt4f high-resolution XPS spectra of **IMIS-PMO-PtCl₂** (Figure 1b) revealed two groups of peaks. These include relatively strong peaks at 72.88 (Pt4f 7/2) and 76.08 eV (Pt4f 5/2), which indicated that the platinum primarily existed as Pt⁺² in **IMIS-PMO-PtCl₂**.^[38] In addition, weaker peaks were observed at 75.38 (Pt4f 7/2) and 78.48 eV (Pt4f 5/2), which implied that a minority of the platinum maintained its +4 valence form, in a similar manner as K₂PtCl₆ after immobilization into the PMO structure.^[39] However, after treatment with NaBH₄, all of the platinum in the **IMIS-PMO-PtCl₂** framework had been reduced to its zero valence form, as only a doublet at 71.68 (Pt4f 7/2) and 74.78 eV (Pt4f 5/2) could be found in this case (Figure 1c).^[40] The slight shift in the binding energy can be attributed to the interaction between Pt and N atoms or Pt and the C=N double bonds, which can also be proven by the presence of the peak at 401.79 eV in the N1s high-resolution XPS spectra of **IMIS-PMO-Pt(0)** (Figure 1d).^[38]

FIGURE 1 XPS survey spectrum of **IMIS-PMO-Pt(0)** (a). Also shown are high-resolution Pt4f XPS spectra of **IMIS-PMO-PtCl₂** (b) and **IMIS-PMO-Pt(0)** (c) before use as catalysts as well as the high-resolution N1s XPS spectrum of **IMIS-PMO-Pt(0)** (d)



Lastly, the exact platinum content in **IMIS-PMO-Pt(0)** was determined by ICP, and was found to be 7.27 wt%. This value suggested that merely one quarter of the IMIS moieties (probably those distributed on the superficial layer of the pore walls) were chelated with platinum, whilst almost three quarters of the IMIS units were inaccessible in the PMO matrix (calculating method see SI).

3.1.2 | Microstructure and surface morphology characterization of **IMIS-PMO**, **IMIS-PMO-PtCl₂**, and **IMIS-PMO-Pt(0)**

The mesoporous microstructures of **IMIS-PMO** series were demonstrated by N₂ adsorption analysis (Figure 2) and TEM characterization. The surface area of each sample was calculated via the BET method (See Table S1 in the SI).^[41] The surface area of **IMIS-PMO** series decreased drastically when the platinum chloride was introduced into the matrix, and it further diminished when the platinum was reduced to its zero-valence state. The shape of the hysteresis loop with p⁰/p ranging from 0.45 to 0.95 indicated that ink-bottle-shaped pore structures were presented inside the materials, and the small distributions at around 3.8 nm of all three plots, which were calculated by BJH method using the adsorption curves in Figure 2b, were artefacts of the closure of the hysteresis. The broad peaks in Figure 2(b), which started from about

5 nm and ended at over 20 nm, should be due to the packing spaces between small particles with rough surfaces and generally small dimensions (about 100 to 150 nm in diameter, see Figure 3a). However, the true inner pore structures could be clearly seen from the TEM image of **IMIS-PMO** (Figure 3b), presenting uniform mesoporous channels (with diameter of 4–5 nm) which were comparable to most periodic mesoporous organosilica frameworks prepared using CTAB as a template.^[42] The well-ordered pore channels could also be proven by the low angle XRD pattern of **IMIS-PMO-Pt(0)** and **IMIS-PMO-PtCl₂**, in which there were peaks at 2 θ = 1.04° for (100) diffraction (Figure S12, SI).

The platinum distribution throughout the **IMIS-PMO** framework was also investigated via TEM methods. As shown by the STEM image of **IMIS-PMO-PtCl₂** (Figure 3c), the Pt(II) complexes were uniformly distributed throughout the silica matrix, mainly as small nanoclusters with diameters of less than 1 nm. In the case of **IMIS-PMO-Pt(0)**, the larger platinum(0) nanocrystals with diameters in the range of 1–2 nm could be clearly observed in the corresponding TEM image (Figure 3d). Furthermore, the formation of platinum(0) nanocrystals can be proven by the HRTEM image (Figure 3e) of one of these platinum crystals showing the lattice fringes,^[43] and also by the XRD pattern of **IMIS-PMO-Pt(0)** (Figure S11 in the SI), in which four diffraction peaks were identical to the characteristic diffraction lines of platinum crystals.^[44]

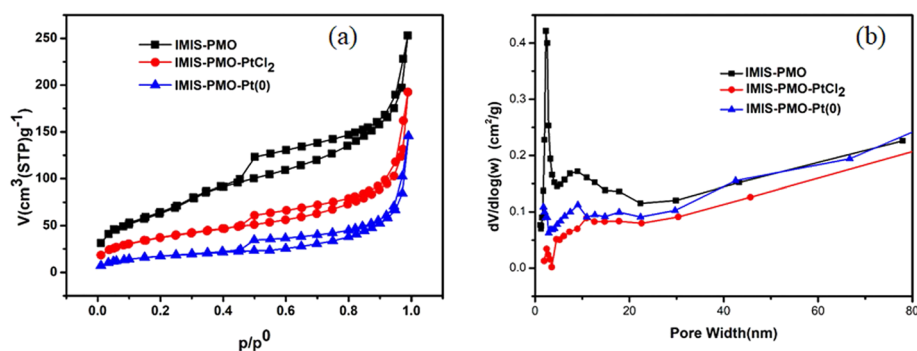


FIGURE 2 N₂ adsorption/desorption isotherms (a) and pore size distributions (b) of IMIS-PMO, IMIS-PMO-PtCl₂, and IMIS-Pt(0)

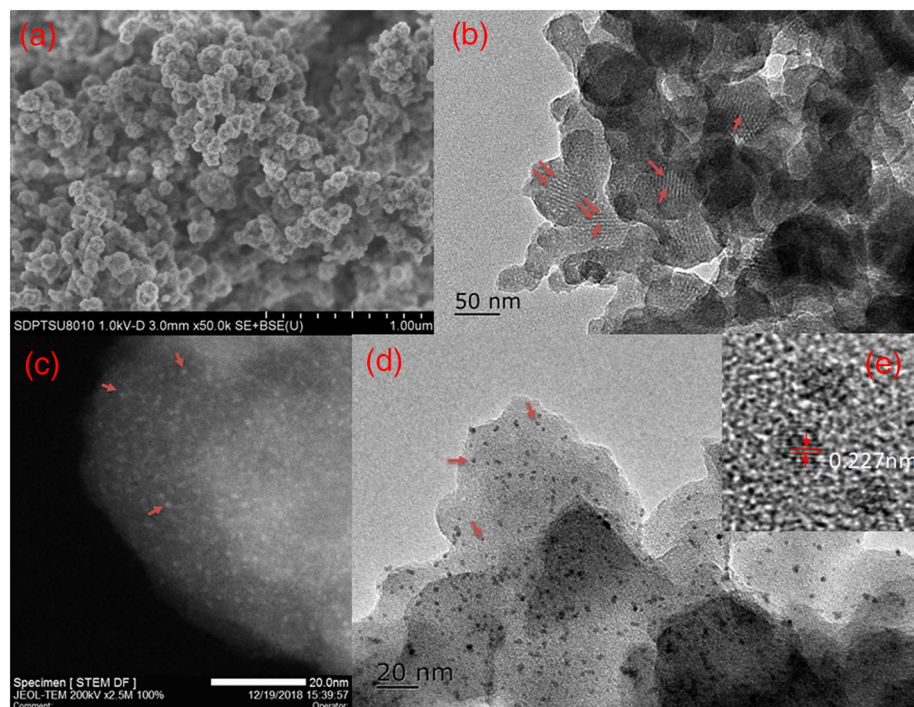


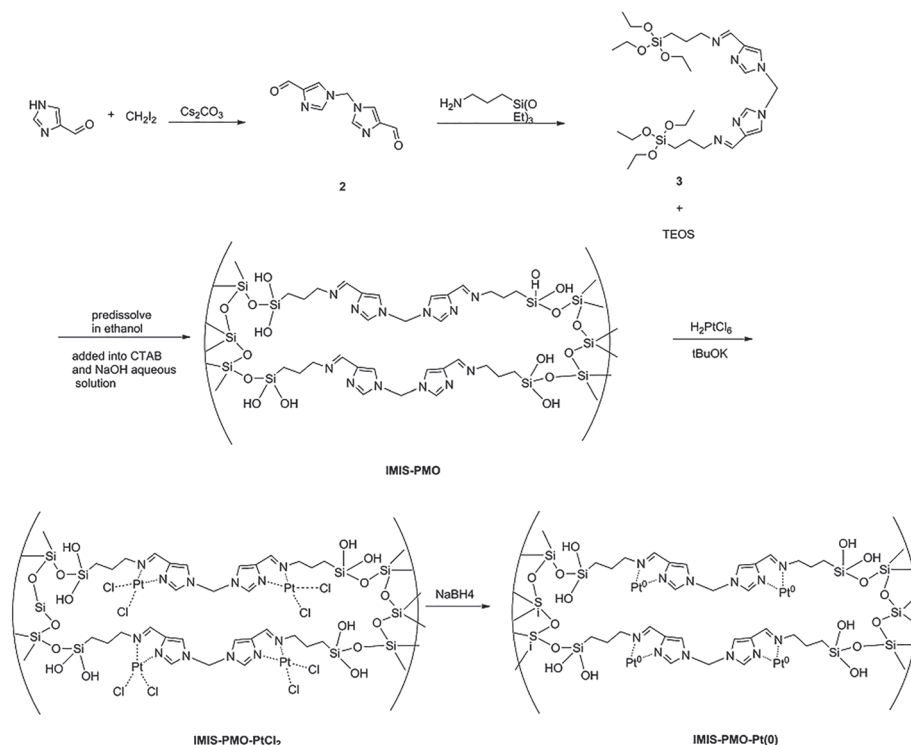
FIGURE 3 SEM image of IMIS-PMO (a), TEM image of IMIS-PMO (b), STEM image of IMIS-PMO-PtCl₂ (c), TEM image of IMIS-PMO-Pt(0) (d), and an HRTEM of platinum nanoparticles in IMIS-PMO-Pt(0) (e)

3.2 | Application of IMIS-PMO-Pt in hydrosilylation reactions

The performances of IMIS-PMO-PtCl₂ and IMIS-PMO-Pt(0) as catalysts for hydrosilylation reactions were evaluated on account of their ability to mediate a model reaction between 1-octene and triethoxysilane (Scheme 2). The influence of the catalyst dosage on the hydrosilylation reaction was examined first. The results are listed in Table 1 as entries 1–4, together with the corresponding reaction conditions. In the case of **IMIS-PMO-PtCl₂**, when 5 mmol of 1-octene was treated with an equal amount of silane for 6 hr at 60 °C, a 98.0% conversion of 1-octene could be achieved (calculated by ¹H NMR) when 3.2 mg of this catalyst (0.0250 mol% of Pt, see entry 2) was used. When 3.1 mg of **IMIS-PMO-Pt(0)** (0.0232 mol% of Pt) was used as a catalyst, the conversion reached as high as 99.5% (Table 1, entry 4) under the

same reaction conditions as those employed for entry 2. Increasing the catalyst dosages resulted in a minor increase in the conversion percentage (see entries 1 and 3).

The effect of the reaction time (Table 1, entries 4–8) and reaction temperature (Table 1, entries 4, 8–11) on hydrosilylation reactions that were mediated by IMIS-PMO-Pt(0) were then studied. Samples were collected for ¹H NMR analysis at 0, 0.5, 1, and 2 hr during the reaction and the conversion rates of 1-octene at each interval were then calculated. The conversion rate increased dramatically as the reaction progressed, and it exceeded 99.0% after 2 hr. The reaction could only be activated when the reaction temperature exceeded 60 °C, and could not proceed at low temperatures. Furthermore, it was found that excellent regioselectivities were achieved through the ¹H NMR spectra of the final products in most cases, as no alpha adducts could be found. Yet it has to be noted that

SCHEME 2 Modeling hydrosilylation reaction**TABLE 1** Data collected during various hydrosilylation tests with **IMIS-PMO-PtCl₂** and **IMIS-PMO-Pt(0)**

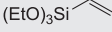
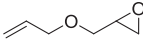
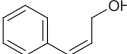
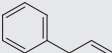
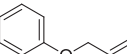
entry	catalyst	Catalyst amount (mg)	Pt amount (mmol)	Pt dosage (mol%)	Temperature (°C)	Conversion % ^a	TOF h ⁻¹	TON
1	IMIS-PMO-PtCl₂	30.1	0.0117	0.234	60 (6 h)	>99.5	71	427
2	IMIS-PMO-PtCl₂	3.2	0.00125	0.0250	60 (6 h)	98.0	667	4000
3	IMIS-PMO-Pt(0)	30.2	0.0113	0.226	60 (6 h)	>99.5	74	442
4	IMIS-PMO-Pt(0)	3.1	0.00116	0.0232	60 (6 h)	99.5	718	4310
5	IMIS-PMO-Pt(0)	3.1	0.00116	0.0232	60 (0 h)	0	/	/
6	IMIS-PMO-Pt(0)	3.1	0.00116	0.0232	60 (0.5 h)	35.5	3060	1530
7	IMIS-PMO-Pt(0)	3.1	0.00116	0.0232	60 (1 h)	94.8	4086	4086
8	IMIS-PMO-Pt(0)	3.1	0.00116	0.0232	60 (2 h)	>99.0	2160	4310
9	IMIS-PMO-Pt(0)	3.0	0.00112	0.0224	20 (2 h)	0	/	/
10	IMIS-PMO-Pt(0)	3.2	0.00119	0.0238	40 (2 h)	0	/	/
11	IMIS-PMO-Pt(0)	3.1	0.00116	0.0232	80 (2 h)	>99.5	2160	4310

^aConditions: 1-Octene was mixed with a set amount of catalyst in a 25 ml flask and preheated at given temperature for 0.5 hr. Triethoxyl hydrosilane was then added to the mixture and the reaction was allowed to proceed for another 2–4 hr. The conversion% were calculated via ¹H NMR characterization using CDCl₃ as a solvent.

trace amount of 2-Octene and n-octane could also be identified in the final products. The ability of **IMIS-PMO-Pt(0)** to mediate hydrosilylation reactions involving various substrates was then evaluated by using various substituted olefins and styrenes. As can be seen in Table 2, in most cases, **IMIS-PMO-Pt(0)** exhibited positive catalytic activity, and the impressive selectivity was retained. In cases involving the olefins bearing a terminal alkene such as 1-octene (Table 1, entry 9), 1-octadecene

(Table 2, entry 1), triethoxy (vinyl)silane (Table 2, entry 2), and (vinyloxy)benzene (Table 2, entry 9), all of the conversion% were over 99%, which indicated that the catalyst had high activity for hydrosilylation reactions. When the olefins contained other functional groups, moderate to high conversion percentages could also be obtained (See Table 2, entries 3, 6, and 7). Meanwhile, when the **IMIS-PMO-Pt(0)** was used to mediate the hydrosilylation between styrene and triethoxysilane, the

TABLE 2 Catalytic activity of **IMIS-PMO-Pt(0)** for the hydrosilylation of various olefins with triethoxysilane^a

Entry	Olefin	Silane	Reaction temperature (°C)	Reaction time (hr)	Conversion%	Selectivity (β-/α- adduct percentage)	TOF (h ⁻¹)
1	 C ₁₆ H ₃₃	HSi (OEt) ₃	60	2	98.3	mainly β-adduct ^b	2118
2	 (EtO) ₃ Si	HSi (OEt) ₃	60	2	99.2	Only β-adduct	2138
3		HSi (OEt) ₃	60	2	90.9	Only β-adduct	1959
4	 (OMe) ₂ Si	HSi (OEt) ₃	60	2	83.4	Only β-adduct	1797
5		HSi (OEt) ₃	60	2	88.4	5:1	1905
6		HSi (OEt) ₃	60	2	81.5	Only β-adduct	1756
7		HSi (OEt) ₃	60	2	37.5	Only α-adduct	808
8		HSi (OEt) ₃	60	2	42.9	Only β-adduct	924
9		HSi (OEt) ₃	60	2	>99.5	Only β-adduct	2155
10		HSi (OEt) ₃	60	2	41.2	Only β-adduct	888

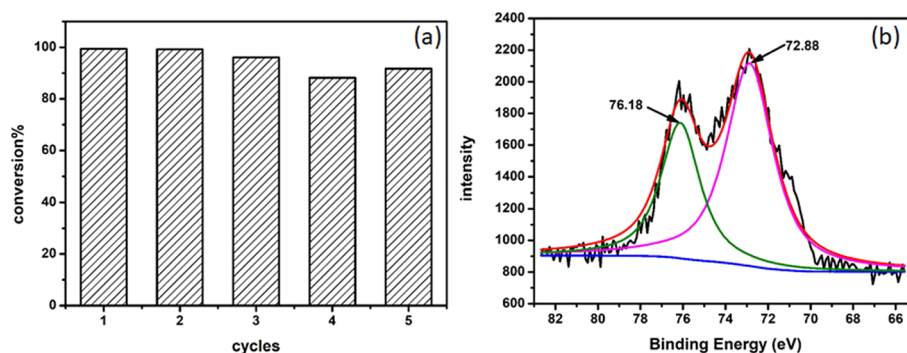
^aThe platinum dosage was set at 0.0232 mol% (in comparison with moles of the olefin), while the olefin:silane molar ratio was 1:1.

^bNo alpha adducts could be found, but trace amount of 2-octadecene and n-octadecane could possibly exit.

conversion could reach 80.1%, which was comparable to most catalysts reported in the literature.^[45] In addition, the β-/α- adduct percentage was ~ 5:1, according to the

¹H NMR data. As shown in entry 8, table 2, the conversion% of 4-Phenyl but-1-ene was relatively low when catalyzed by **IMIS-PMO-Pt(0)**, comparing to that catalyzed

FIGURE 4 Recycling experiments with **IMIS-PMO-Pt(0)** (a) and high-resolution XPS spectra of Pt4f in **IMIS-PMO-Pt(0)** after 5 cycles (b)



by the Kardert's catalyst,^[46] and this might be a result of lower reaction temperature and shorter reaction time in this research.

Finally, the recyclability of **IMIS-PMO-Pt(0)** was also investigated. As shown in Figure 4a, the catalyst can be used in five consecutive runs without exhibiting significant loss in activity. Yet according to the high-resolution Pt4f XPS spectra of the catalyst after five reaction cycles (Figure 4b), the platinum was oxidized to its +2 valence state, and its catalytic activity toward hydrosilylation reactions was still retained. We suspected that the catalyst was gradually oxidized through the reaction procedure, and further investigation into the catalytic mechanism is still underway. In conclusion, the **IMIS-PMO-Pt(0)** can be used as an efficient catalyst for hydrosilylation reactions.

4 | CONCLUSION

In conclusion, we have prepared an imidazolyl Schiff base containing periodic mesoporous organosilica (PMO) framework via co-condensation reactions between a newly synthesized bis (imidazolyl)imine-bridged bis silane and tetraethyl orthosilicate, with cetyltrimethyl ammonium bromide serving as a soft template. The synthesized PMO framework can serve as a solid support for platinum complexes and nanoparticles as the chelating imidazolyl imine moieties are uniformly distributed within the pore walls without blocking the meso pores. The resulting catalyst can efficiently mediate hydrosilylation reactions between olefins and hydrosilanes, and it can be reused for at least five cycles without significant loss of activity.

ACKNOWLEDGMENTS

The authors wish to thank the National Natural Science Foundation of China (51173204, 51503124, 21404121, and 21404122), the Guangdong Natural Science Foundation (2018A030313946), the Production Education Research Project in Guangdong Province

(2015B090915004), the Science and Technology Program of Guangzhou City (201802010018, 201904020019), and the Sichuan Science and Technology Project (2019YFSY0011) for providing financial support. We are also grateful for the support provided by the Innovative Talents Youth Program (Natural Science) in Universities of Guangdong (2017-GKQNC113), and the Guangzhou Industrial Technology Major Project (201802010018).

ORCID

Jiwen Hu  <https://orcid.org/0000-0002-8473-5797>

REFERENCES

- [1] B. Marciniec, H. Maciejewski, C. Pietraszuk, P. Pawl, *Advances in Silicon Science-Hydrosilylation: A Comprehensive Review on Recent Advances*, Springer, Netherlands **2009**.
- [2] J. L. Speier, J. A. Webster, G. H. Barnes, *J. Am. Chem. Soc.* **1957**, 79, 574.
- [3] B. D. Karstedt, USA, 3775452. **1973**.
- [4] I. E. Marko, S. Sterin, O. Buisine, G. Mignani, P. Branlard, B. Tinant, J. P. Declercq, *Science* **2002**, 298, 204.
- [5] M. Okamoto, H. Kiya, H. Yamashita, E. Suzuki, *Chem. Commun.* **2002**, 15, 1634.
- [6] H. Bai, *Ind. Eng. Chem. Res.* **2012**, 51, 16457.
- [7] M. Pagliaro, R. Ciriminna, V. Pandarus, F. Béland, *Eur. Org. Chem.* **2013**, 28, 6227.
- [8] N. Mizoshita, T. Tania, S. Inagaki, *Chem. Soc. Rev.* **2011**, 40, 789.
- [9] C. Yu, J. Shi, *Adv. Mater.* **2016**, 28, 3235.
- [10] P. Van Der Voort, D. Esquivel, E. De Canck, F. Goethals, I. Van Driessche, F. J. Romero-Salguero, *Chem. Soc. Rev.* **2013**, 42, 3913.
- [11] W. Wang, J. E. Lofgreen, G. A. Ozin, *Small* **2010**, 6, 2634.
- [12] S. S. Park, M. S. Moorthy, C.-S. Ha, *Korean J. Chem. Eng.* **2014**, 31, 1707.
- [13] M. Waki, N. Mizoshita, T. Tani, S. Inagaki, *Angew. Chem. Int. Ed.* **2011**, 50, 11667.
- [14] X. Zhang, Y. Huang, Y. Guo, X. Yuan, F. Jiao, *Micropor. Mesopor. Mater.* **2018**, 262, 251.
- [15] F. Lin, X. Meng, E. Kukueva, T. Altantzis, M. Mertens, S. Bals, P. Coola, S. Van Doorslaer, *Dalton Trans.* **2015**, 44, 9970.
- [16] X. Liu, Y. Maegawa, Y. Goto, K. Hara, S. Inagaki, *Angew. Chem. Int. Ed.* **2016**, 55, 1.

- [17] A. Ishikawa, Y. Maegawa, M. Waki, S. Inagaki, *ACS Catal.* **2018**, *8*, 4160.
- [18] K. C. Gupta, A. K. Sutar, *Coord. Chem. Rev.* **2008**, *252*, 142.
- [19] T. N. Sorrell, M. L. Garrity, *Inorg. Chem.* **1991**, *30*, 210.
- [20] K. Shankar, J. B. Baruah, *Z. Anorg. Allg. Chem.* **2015**, *641*, 2558.
- [21] Y. Sunatsuki, Y. Motoda, *Coord. Chem. Rev.* **2002**, *226*, 199.
- [22] E. Mijangos, J. Reedijk, L. Gasque, *Dalton Trans.* **2008**, 1857.
- [23] M. L. Branham, P. Singh, K. Bisetty, M. Sabela, T. Govender, *Molecules* **2011**, *16*, 10269.
- [24] V. R. Souza, H. R. Rechenberg, J. A. Bonacin, H. E. Toma, *Spectrochim. Acta Part A* **2018**, *71*, 1296.
- [25] P. Cañellas, M. Torres, A. Bauzá, M. M. Cánaves, K. Sánchez, M. I. Cabra, A. García-Raso, J. J. Fiol, P. M. Deyà, E. Molins, I. Mata, A. Frontera, *Eur. J. Inorg. Chem.* **2012**, 3995.
- [26] K. Li, J.-L. Niu, M.-Z. Yang, Z. Li, L.-Y. Wu, X.-Q. Hao, M.-P. Song, *Organometallics* **2015**, *34*, 1170.
- [27] M. Safa, R. J. Puddephatt, *J. Organomet. Chem.* **2014**, *761*, 42.
- [28] C. Egloff, R. Gramage-Doria, M. Jouffroy, D. Armspach, D. Matt, *C. R. Chimie* **2013**, *16*, 509.
- [29] Y.-M. Ho, C.-K. Koo, K.-L. Wong, H.-K. Kong, C. T.-L. Chan, W.-M. Kwok, C.-F. Chow, M. H.-W. Lam, W.-Y. Wong, *Dalton Trans.* **2012**, *41*, 1792.
- [30] T. Janine, *J. Organomet. Chem.* **2004**, *689*, 1315.
- [31] Y. Naganawa, Y. Maegawa, H. Guo, S. S. Gholap, S. Tanaka, K. Sato, S. Inagaki, Y. Nakajima, *Dalton Trans.* **2019**, *48*, 5534.
- [32] M. Yoshida, K. Saito, H. Matsukawa, S. Yanagida, M. Ebina, Y. Maegawa, S. Inagaki, A. Kobayashi, M. Kato, *Photocatalysis* **2018**, *358*, 334.
- [33] B. Karimi, Z. Naderi, M. Khorasani, H. M. Mirzaei, H. Vali, *ChemCatChem* **2016**, *8*, 906.
- [34] F. Zhua, D. Yang, F. Zhang, *J. Mol. Catal. A: Chem.* **2012**, *363*, 387.
- [35] D. Zhang, T. Cheng, G. Liu, *Appl. Catal. B: Environ.* **2015**, *174*, 344.
- [36] M. K. Dinker, P. S. Kulkarni, *Micropor. Mesopor. Mater* **2016**, *230*, 145.
- [37] P. Pospiecha, J. Chojnowski, U. Mizerska, T. Makowski, K. Strzelec, N. Sienkiewicz, *Appl. Organomet. Chem.* **2016**, *30*, 399.
- [38] P. Brant, J. H. Enemark, A. Balch, *J. Organomet. Chem.* **1976**, *114*, 99.
- [39] C. Battistoni, A. M. Giuliani, E. Paparazzo, F. Tarli, *J. Chem. Soc., Dalton Trans.* **1984**, *0*, 1293.
- [40] H. Zai, Y. Zhao, S. Chen, L. Ge, C. Chen, Q. Chen, Y. Li, *Nano Res.* **2018**, *11*, 2544.
- [41] Y. Yang, Y. Zhang, S. Hao, Q. Kan, *J. Colloid Interface Sci.* **2011**, *362*, 157.
- [42] Y. Huo, J. Hu, S. Lin, J. Xingming, Y. Wei, Z. Huang, Y. Hu, T. Yuanyuan, *Appl. Organomet. Chem.* **2019**, *33*, 4874.
- [43] G. Yang, Y. Wei, Z. Huang, J. Hu, G. Liu, O. Ming, S. Lin, T. Yuanyuan, *ACS Appl. Mater. Interfaces* **2018**, *10*, 6778.
- [44] L. Yang, N. Chen, F. Wang, Y. Cai, H. Zhu, *New J. Chem.* **2017**, *41*, 6585.
- [45] J. Peng, Y. Bai, J. Li, G. Lai, *Curr. Org. Chem.* **2011**, *15*, 2802.
- [46] Z. Pan, M. Liu, C. Zheng, D. Gao, W. Huang, *Chin. J. Chem.* **2017**, *35*, 1227.

SUPPORTING INFORMATION

Additional supporting information may be found online in the Supporting Information section at the end of this article.

How to cite this article: Huo Y, Hu J, Tu Y, et al. Platinum-Imidazolyl Schiff Base Complexes Immobilized in Periodic Mesoporous Organosilica Frameworks as Catalysts for Hydrosilylation. *Appl Organomet Chem.* 2020;e5697. <https://doi.org/10.1002/aoc.5697>